NATIONAL ADVISORY COMMITTEE FOR AERONAUTICS

TECHNICAL NOTE 3813

COMPARISON OF THEORETICAL STRESSES AND DEFLECTIONS OF MULTICELL WINGS WITH EXPERIMENTAL RESULTS OBTAINED FROM PLASTIC MODELS

By George W. Zender

Langley Aeronautical Laboratory
Langley Field, Va.

Washington
November 1956

L

NATIONAL ADVISORY COMMITTEE FOR AERONAUT

TECHNICAL NOTE 3813

COMPARISON OF THEORETICAL STRESSES AND DEFLECTIONS OF MULTICELL WINGS WITH EXPERIMENTAL RESULTS OBTAINED FROM PLASTIC MODELS

By George W. Zender

SUMMARY

The experimental deflections and stresses of six plastic multicell-wing models of unswept, delta, and swept plan form are presented and compared with previously published theoretical results obtained by the electrical analog method. The comparisons indicate that the theory is reliable for evaluating deflections. In addition, the model tests indicate that the theory is reliable for stresses except near the leading edge of the delta wings and the leading and trailing edges of the swept wings where the simplifications employed in idealizing the actual structure and local effects of the concentrated loading introduce appreciable errors.

INTRODUCTION

In a recent series of papers (refs. 1, 2, and 3), Benscoter and McNeal presented the theoretical structural analysis of low-aspect-ratio multicell-wing designs of unswept, swept, and delta plan form. In these papers, stress and deflection results were obtained by the electrical analog method (ref. 4) for eight different sample wings. No experimental check was made, however, on the validity of the results which necessarily involved a number of simplifying assumptions. The purpose of the present paper is to present and compare companion experimental results obtained from plastic models geometrically similar to the wings used in references 1 to 3.

The use of scaled plastic models is an attractive approach for experimental deflection and stress determination. Not only are such models inexpensive but they can also be constructed quickly and tested with relatively simple experimental equipment. Although this saving in time and cost is probably obtained with a sacrifice in accuracy and quantity of useful information, it is felt that these disadvantages can be minimized by proper and careful testing. The experimental results should therefore provide a satisfactory basis for assessing the

theoretical results. In addition, the comparisons between theory and experiment contained herein should provide an indirect validation of the test procedure using plastic models.

TEST SPECIMENS

Six plastic models, geometrically similar to the prototype multicell-wing designs presented in references 1, 2, and 3, were constructed of clear Plexiglas I-A sheet material to the dimensions shown in figures 1, 2, and 3. A scale factor of 3/8 was selected in order that the thinnest standard gage of Plexiglas I-A sheet material (0.06 inch) could be used for the covers which were 0.16 inch thick for the prototype wings. The nonstandard thicknesses of the spars and ribs were obtained by machining standard-gage sheet material to the proper thickness. As a consequence, the spar and rib thicknesses did not vary appreciably from the design values; whereas, thickness measurements obtained on the covers of the models ranged from 0.05 to 0.07 inch as compared with the nominal value of 0.06 inch. In order to delay buckling of the covers of the relatively large square cells of the delta and swept models with rectangular cross sections (figs. 2(a) and 3(a)), $\frac{1}{4}$-inch-square posts were located at the center of the cells as shown in figure 4. The joints of the spars, ribs, and covers were attached with Cement I-A and the models were allowed to age as indicated in reference 5 in order to avoid appreciable changes in the stiffness of the models during the course of the tests.

METHOD OF TESTING

The test setups of the delta-wing models are shown in figures 4 and 5. Figure 5 shows the delta-wing model of biconvex cross section which was supported at the ends of the carrythrough section by a frame made of $\frac{1}{2}$-inch-thick mahogany fitted to the contour of the wing and tapered in thickness to approximately $\frac{1}{16}$ inch in width at the line of contact of the frame with the model. This method of support was also used for the unswept and swept models of biconvex cross sections. The models with rectangular cross sections were supported by 1-inch-diameter drill rods as shown in figure 4. Dead weights were used to apply loads to the models and the loads were transmitted to the plastic model through 1- by 1-inch aluminum plates padded with rubber on the side adjacent to the wing. In order to apply twisting loads, the trailing-edge tip of the models was loaded downward and the leading-edge tip was

loaded upward by means of piano wire which was suspended over a pulley above the model and supported dead weights at the opposite end of the wire.

Although a number of investigators have reported techniques applied in obtaining the deflections of plastic models, considerably less information is available about methods which are satisfactory for obtaining the stresses of such models. In reference 6, techniques are discussed which were applied in obtaining strains or stresses from a plastic model of a delta-wing airplane; and references 7, 8, and 9 present some information concerning strain measurements in small strips or standard tensile specimens made of plastic material. In order to establish a reliable technique to be used in obtaining strain measurements on the plastic multicell wing models, tests were performed on elementary-type box beams constructed of Plexiglas I-A sheet material and the results of these tests were reported in reference 10. On the basis of the information presented in reference 10, the following procedure was used in performing tests on the plastic multicell-wing models. The tests were performed in an air-conditioned room maintained at a temperature of $70^{\circ} \pm 1^{\circ}$ F in order to avoid appreciable changes in material properties due to temperature variations and the large creep effects which occur at higher temperatures. Strain and deflection measurements were obtained for at least four successive increments of load and the maximum stresses in the model were limited to less than 500 psi.

The deflections of the models were obtained with dial gages and the outer surface strains of the covers were measured with Tuckerman optical-type gages. In addition, strain measurements were obtained on some of the vertical shear webs with SR-4 type rosettes.

MATERIAL PROPERTIES AND DATA REDUCTION

In order to convert the measured strains to stresses and also in order to compare the measured and theoretical results, the values of Young's modulus, Poisson's ratio, and the shear modulus are required. The values of Poisson's ratio and Young's modulus (for flexure or compression) given by the manufacturer of the material (see ref. 11) are 0.35 and 400 ksi, respectively, at 25° C or 77° F. These values and a shear modulus of 150 ksi were used herein for convenience of calculation and these values were checked approximately by tests of samples of the material used in the plastic wings.

The method of reducing the experimental data involved plotting the strains and deflections for the various levels of applied load and obtaining influence coefficients of strain or deflection from the slope of straight lines fitted to the test points. Normal stress influence coefficients were obtained from the longitudinal and transverse strain

influence coefficients by using the elementary relationship of plane stresses and strains and the appropriate value of Young's modulus (400 ksi) and Poisson's ratio (0.35). The shear stress influence coefficients were obtained by multiplying the shear strain influence coefficient by the shear modulus. Because of the geometric similarity of the plastic models and the prototype wings, the experimental stress and deflection influence coefficients may be adjusted by means of similarity factors for purposes of comparison with the theoretical results given in references 1 to 3. For this purpose, the experimental stress influence coefficients were multiplied by the square of the scale factor (0.375^2), and the experimental deflection coefficients were multiplied by the product of the scale factor and the ratio of the values of Young's modulus of the model to that of the prototype $\left(0.375\ \frac{400}{10,400}\right)$.

RESULTS

The experimental and theoretical stresses and deflections of the six multicell wings are shown in figures 6 to 11 for three loading cases; cases 1 and 2 are for downward loads at the tip and case 3 is for a tip-twisting type of loading consisting of a downward load at the trailing-edge tip and an upward load at the leading-edge tip. The theoretical deflections were taken directly from tables given in references 1 to 3, and the theoretical stresses were calculated from the bending and twisting moments and the shears listed in tables in the references. (Theoretical values shown for the swept wings for the loading case 3 are not included in reference 3 and were therefore obtained by appropriate super-position of the values given for the case 1 and case 2 loadings.) The theoretical deflections and stresses are given for specific stations on the idealized structure and the curves shown in figures 6 to 11 were simply faired through the values. In most cases both experimental and theoretical deflections and stresses were obtained at homologous positions; however, some experimental shear stresses and leading- and trailing-edge normal stresses are shown in figures 8 to 11 for which theoretical values do not exist. The normal stress along the leading or trailing edges shown in figures 8 to 11 was measured in the direction parallel to the leading- or trailing-edge spar but is plotted in the perpendicular direction in the figures for convenience. Similarly, the shear stresses in the spar webs, which are actually in vertical planes, are plotted in horizontal directions in the figures.

DISCUSSION

Unswept Wings

In general, the theoretical and experimental stresses and deflections of the unswept wings compare favorably. The largest differences occur in the normal stresses along the leading or trailing edges when the load is applied to the tip corners (cases 2 and 3). There is some reason to question the accuracy of the theoretical stresses in these regions. A check of the equilibrium of the theoretical bending and twisting moments and shear forces tabulated in reference 1 revealed an appreciable violation of statics of the leading- or trailing-edge members although the net equilibrium of the full chordwise cross sections is satisfactorily established. The dashed curves near the leading and trailing edges in figures 6(c), 6(d), 7(c), and 7(d) show the results obtained when the normal stresses at the outer spars are adjusted so as to establish equilibrium with shear forces and twisting moments tabulated in reference 1 which were regarded as correct in the calculations. These adjusted stresses should not be regarded as the correct normal stresses since either the bending moments, twisting moments, or the shear forces, or any combination of the three could be responsible for the static unbalance. However, the dashed curves give some indication of the amount by which the theoretical normal stresses at the leading and trailing edges may be in error. In addition, the differences in the theoretical and experimental normal stresses near the vicinity of the load may be due to local effects caused by the concentrated load which often appear in experimental data but are not usually included in theoretical studies. Nevertheless, the overall agreement of the experimental and theoretical results for the unswept wings not only substantiates the theoretical approach (if not all of the detailed results) but also lends confidence in the experimental techniques.

Delta Wings

As in the case of the unswept wings, the overall agreement of the experimental and theoretical results of the delta wings of rectangular and biconvex cross section is favorable especially with regard to deflections. Again, appreciable differences occur in experimental and theoretical normal stresses along the leading and trailing edges. Along the trailing edge, these differences are probably due to the local effects of the concentrated load. (Compare figs. 8(b) and (c).) Along the leading edge the differences are probably due to a combination of this local effect and the errors arising from the method used to idealize the triangular panels of the actual structure in the theoretical analysis.

The details of the structural idealization are given in reference 2; sufficient information for the purposes of this discussion is provided in the sketches shown in figure 12 which compare the covers of the actual structure with the idealized or substitute covers used in the theoretical analysis. The usual methods for idealizing the covers of the square or rectangular cells are employed; that is, the assumption is made that all of the normal stresses are carried by flanges around the periphery of the cells and that the skin panels carry only shear stresses. The normal stresses of the triangular cells are also carried by flanges but the shear strains of the triangular panels are resisted only by truss action of the surrounding flanges; the triangular skin panels are assumed to be void as indicated in figure 12.

The experimental shear stresses which exist in the triangular panels (measured on the plastic models at the centroid of the triangles) are indicated in figures 8 and 9. For the two bending-load cases the experimental shear stresses in the triangular panels are of the same order of magnitude as the shear stresses in the adjacent chordwise square panels; however, the shear stresses in the triangular panels for the twisting loads are very small except in the triangular panel nearest the applied load. The actual shear stresses in the triangular panels possibly account for much of the difference in the experimental and theoretical normal stresses in the vicinity of the triangular panels.

Swept Wings

The modifications made in idealizing the covers of the multicell wings were most severe in the case of the swept wings (see fig. 12); the parallelogram-shaped cells of the actual structure were idealized into square panels and triangular trusses of the same type as were used for the delta substitute structure. In view of these assumptions, considerable variation in the experimental and theoretical results might be expected. Indeed, the theory and experiment (figs. 10 and 11) show more inconsistencies than occurred for the unswept and delta plan-form wings. Nevertheless, the experimental deflections and cover shear stresses are in good agreement with the theoretical results. In addition, the normal stresses in the interior portions of the cover show agreement between experiment and theory. On the other hand, the normal stresses in the region of the leading and trailing edges (both spanwise and parallel to the spars) evidence large disparities. These latter stresses occur in the portions of the idealized structure where the triangular trusses are employed, as was the case for the delta wings. The overall results for the swept wings indicate that, even though the triangular truss-like flanges account for the general behavior of the structure, the actual stress distributions in the region of the leading and trailing edges may differ considerably from the theoretical values.

CONCLUDING REMARKS

A comparison of the experimental deflections and stresses of six plastic models of multicell wings of unswept, delta, and swept plan form with previously published theoretical results obtained by the electrical analog method reveal that the theoretical deflections are satisfactorily verified by the experiment. In addition, the model tests indicate that the theory is reliable for stresses except near the leading edge of delta wings and the leading and trailing edges of swept wings where the simplifications employed in idealizing the actual structure and local effects of concentrated loads introduce appreciable errors.

Langley Aeronautical Laboratory,
National Advisory Committee for Aeronautics,
Langley Field, Va., June 25, 1956.

REFERENCES

1. Benscoter, Stanley U., and MacNeal, Richard H.: Analysis of Straight Multicell Wings on Cal-Tech Analog Computer. NACA TN 3113, 1954. (Tabular data not included in this TN are available on loan from Division of Research Information, NACA, Washington, D. C.)

2. MacNeal, Richard H., and Benscoter, Stanley U.: Analysis of Multicell Delta Wings on Cal-Tech Analog Computer. NACA TN 3114, 1953.

3. MacNeal, Richard H., and Benscoter, Stanley U.: Analysis of Sweptback Wings on Cal-Tech Analog Computer. NACA TN 3115, 1954.

4. Benscoter, Stanley U., and MacNeal, Richard H.: Equivalent Plate Theory for a Straight Multicell Wing. NACA TN 2786, 1952.

5. Meadows, Roscoe, Jr.,: Deflection Tests of Plastic Models. Proc. Soc. Exp. Stress Analysis, vol. VIII, no. 2, 1951, pp. 117-128.

6. Redshaw, S. C., and Palmer, P. J.: The Construction and Testing of a Xylonite Model of a Delta Aircraft. The Aeronautical Quarterly, vol. III, pt. II, Sept. 1951, pp. 83-127.

7. Bruhn, Elmer F.: Tests on Thin-Walled Celluloid Cylinders To Determine the Interaction Curves Under Combined Bending, Torsion, and Compression or Tension Loads. NACA TN 951, 1945.

8. Dietz, A. G. H., and Campbell, W. H.: Bonded Wire Strain Gage Techniques for Polymethyl Methacrylate Plastics. Proc. Soc. Exp. Stress Analysis, vol. V, no. 1, 1947, pp. 59-62.

9. Eney, W. J.: Discussion of Paper Entitled "Bonded Wire Strain Gage Techniques for Polymethyl Methacrylate Plastics." Proc. Soc. Exp. Stress Analysis, vol. V, no. 1, 1947, pp. 63-66.

10. Zender, George W.: Experimental Analysis of Multicell Wings by Means of Plastic Models. NACA RM L55E10b, 1955.

11. Anon.: Plexiglas - Handbook for Aircraft Engineers. Second ed., Rohm & Haas Co. (Philadelphia), 1952.

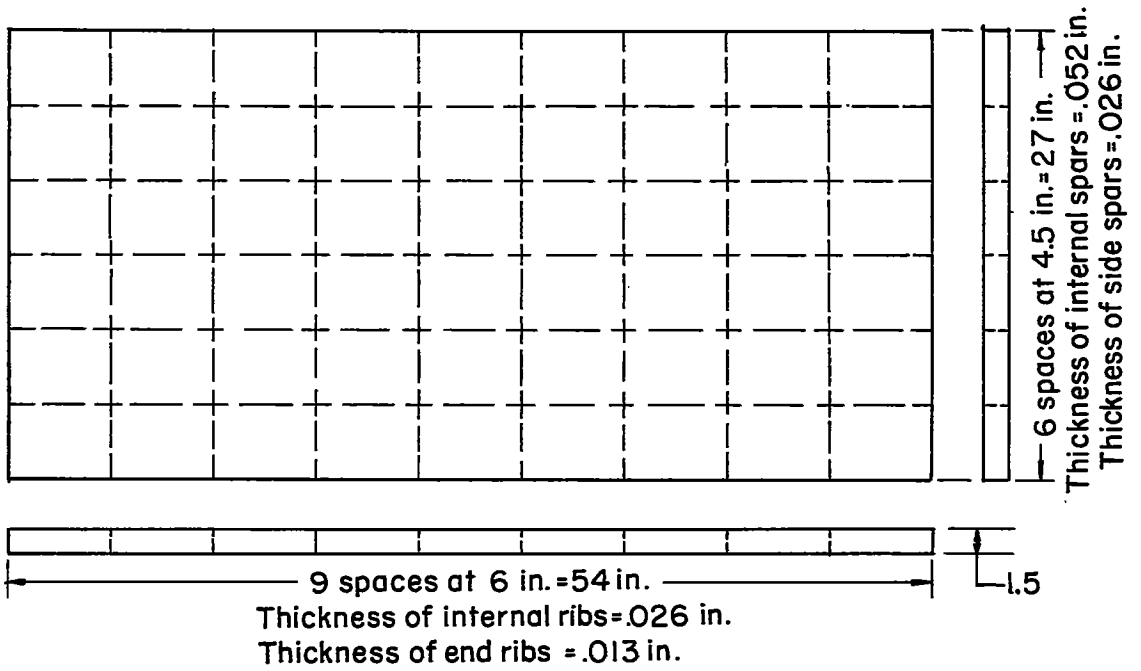

(a) Unswept multicell box beam with rectangular cross section.

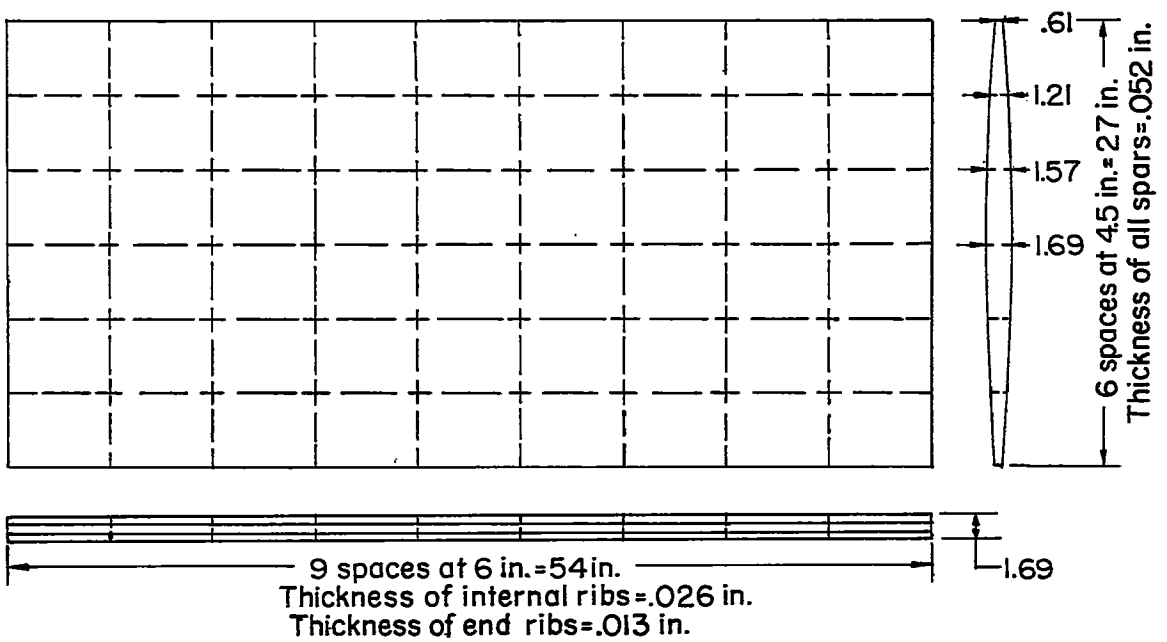

(b) Unswept multicell box beam with biconvex cross section.

Figure 1.- Details of plastic models of unswept plan form. Cover thickness, 0.06 inch.

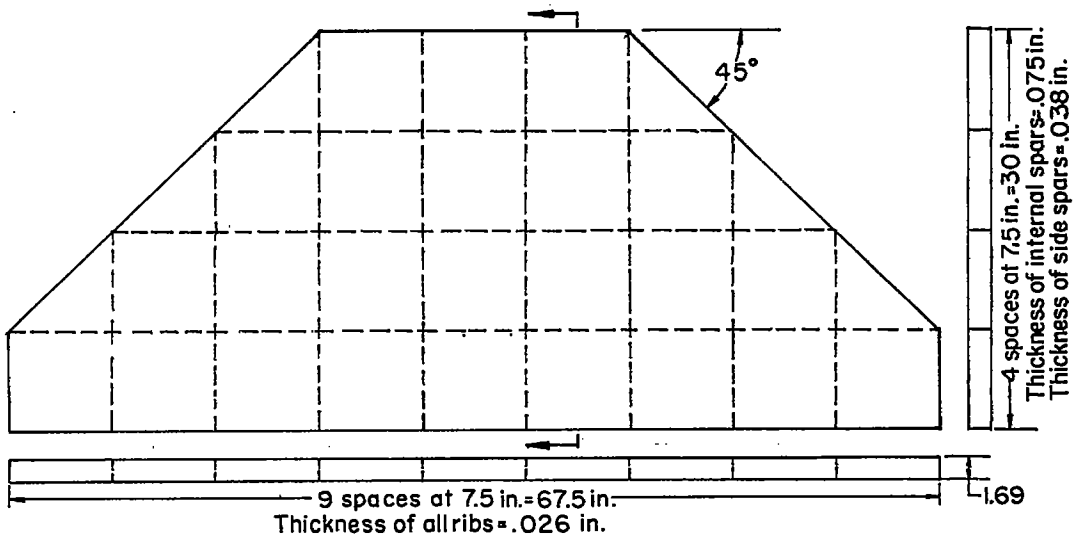

(a) Delta multicell box beam with rectangular cross section.

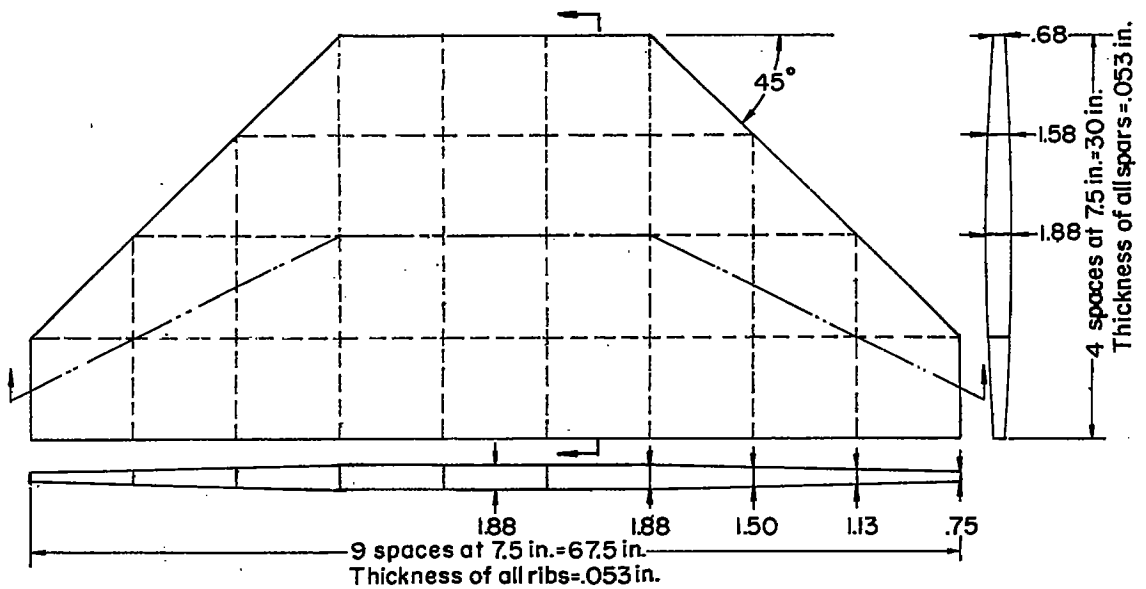

(b) Delta multicell box beam with biconvex cross section.

Figure 2.- Details of plastic models of delta plan form. Cover thickness, 0.06 inch.

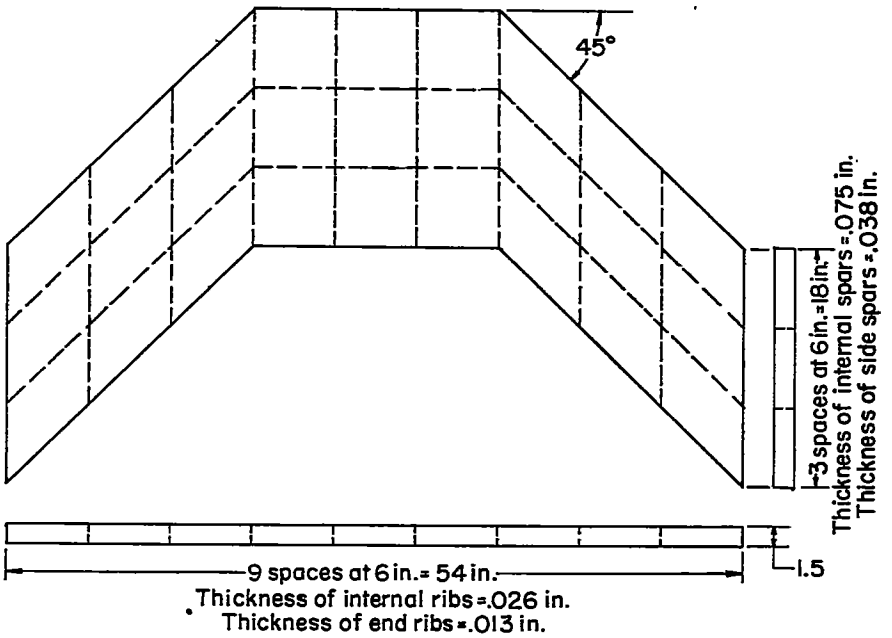

(a) Swept multicell box beam with rectangular cross section.

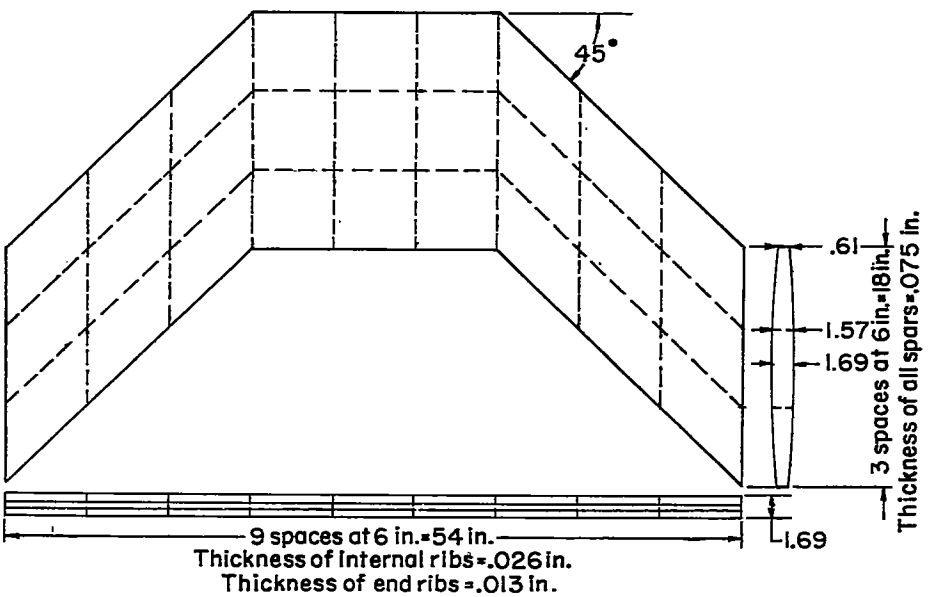

(b) Swept multicell box beam with biconvex cross section.

Figure 3.- Details of plastic models of swept plan form. Cover thickness, 0.06 inch.

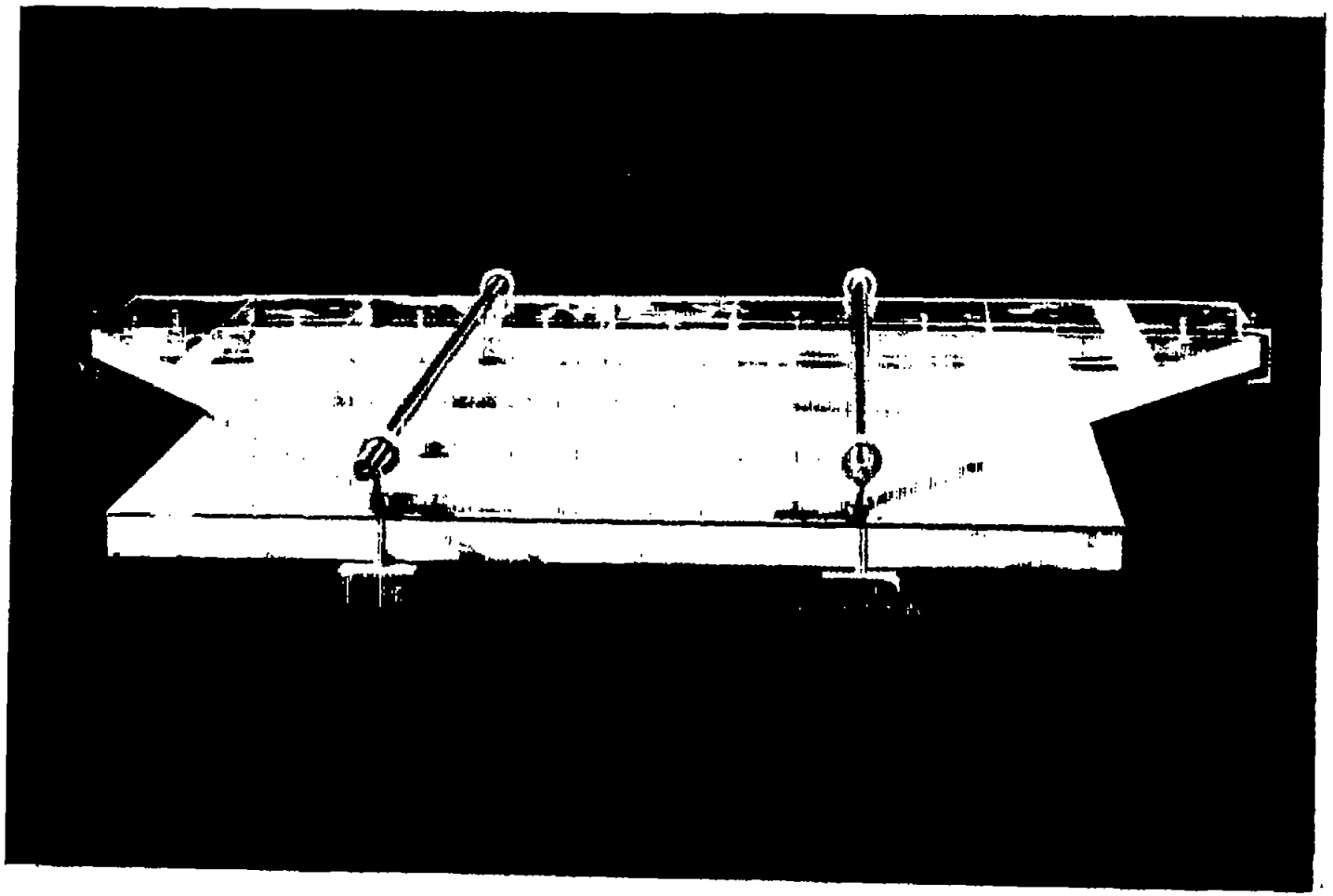

L-86204.1

Figure 4.- Bending test setup of delta-wing model of rectangular cross section.

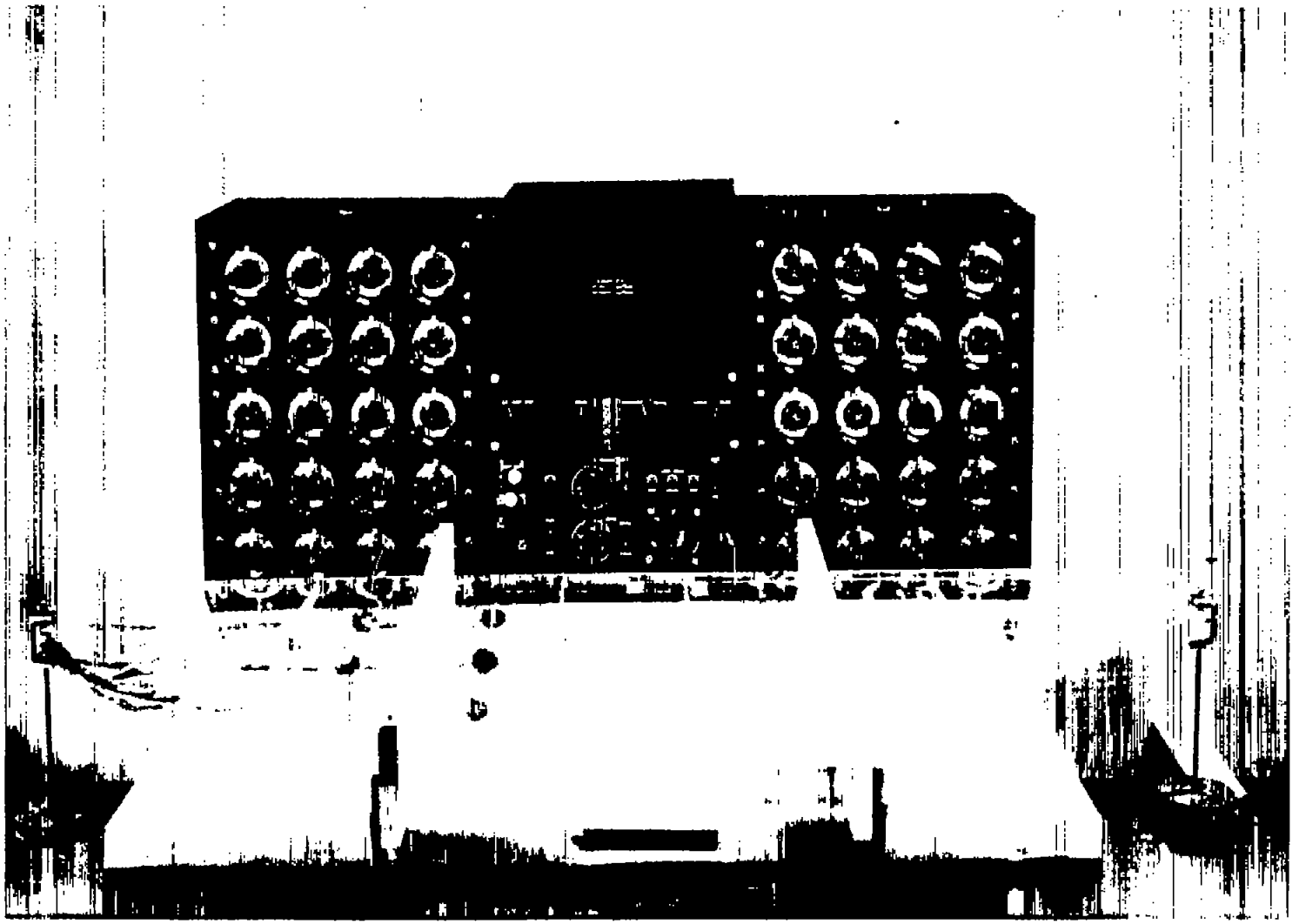

L-90261

Figure 5.- Bending test setup of delta-wing model of biconvex cross section.

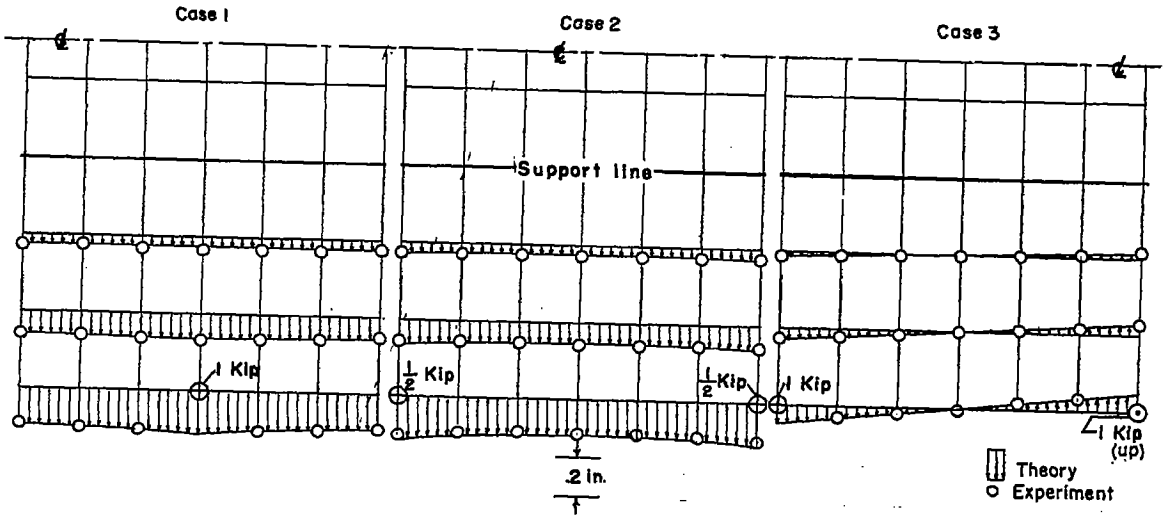

(a) Deflections for bending and twisting loads.

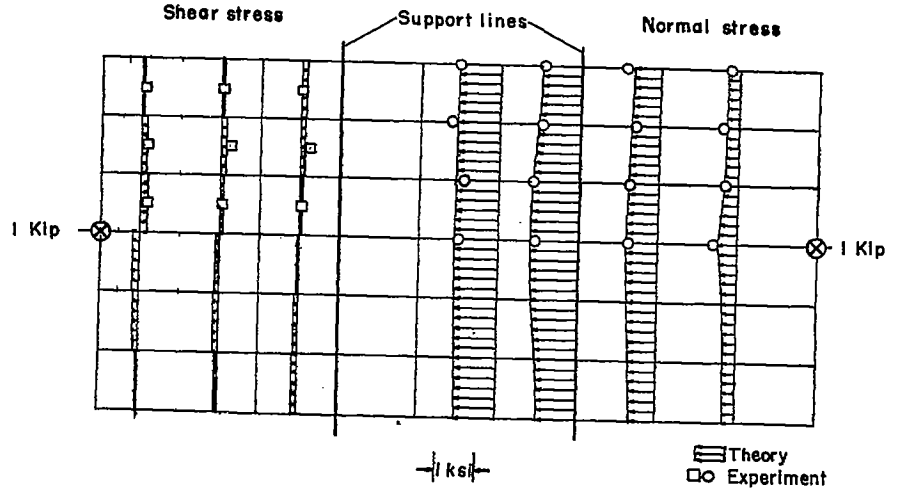

(b) Cover shear and normal stresses for loading case 1.

Figure 6.- Deflections and stresses of unswept wing with rectangular cross section.

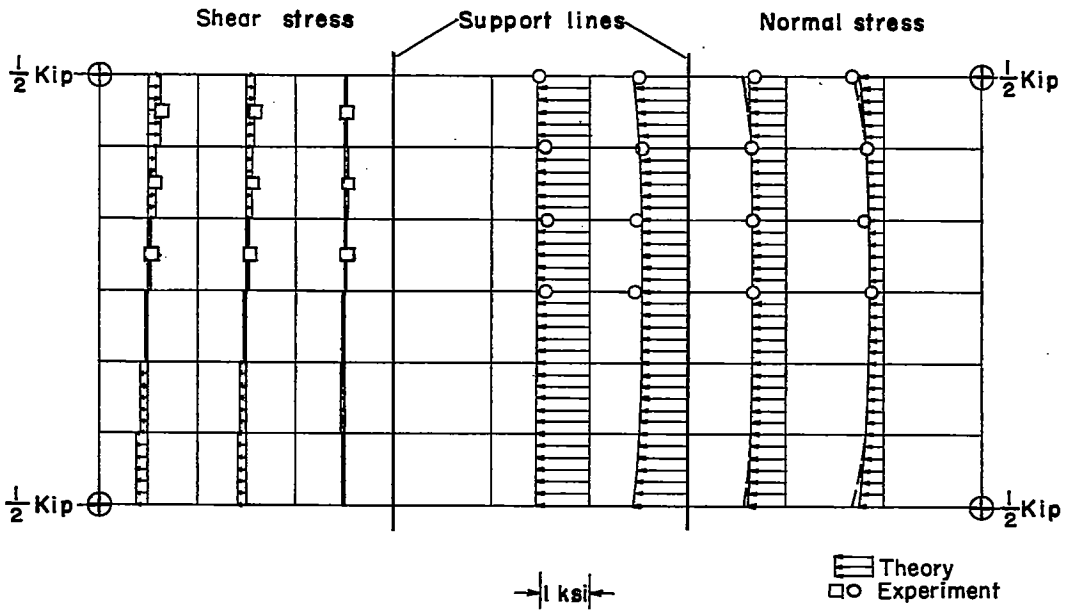

(c) Cover shear and normal stresses for loading case 2.

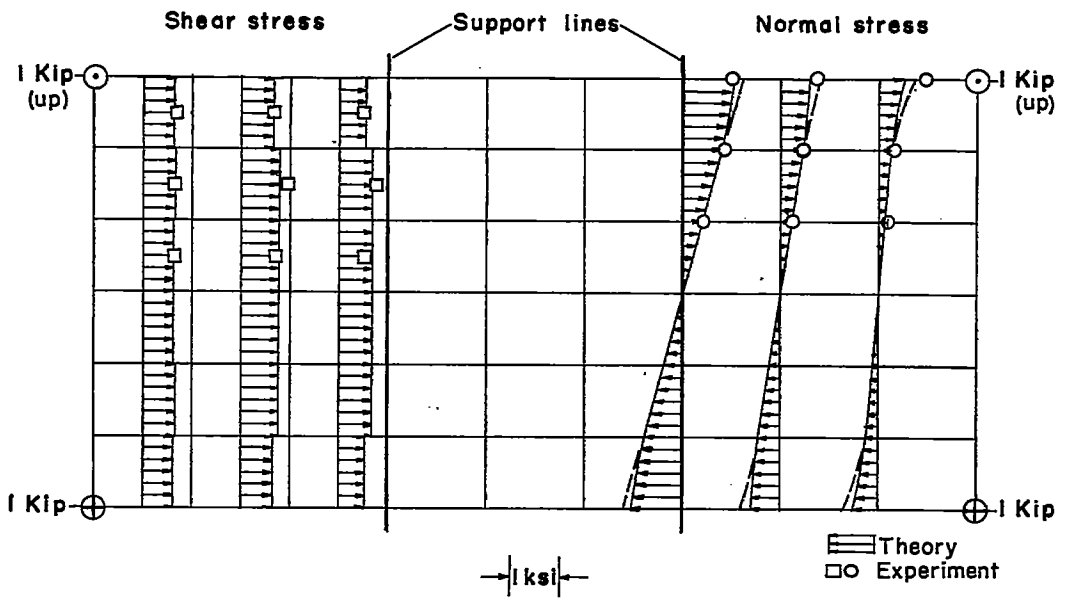

(d) Cover shear and normal stresses for loading case 3.

Figure 6.- Continued.

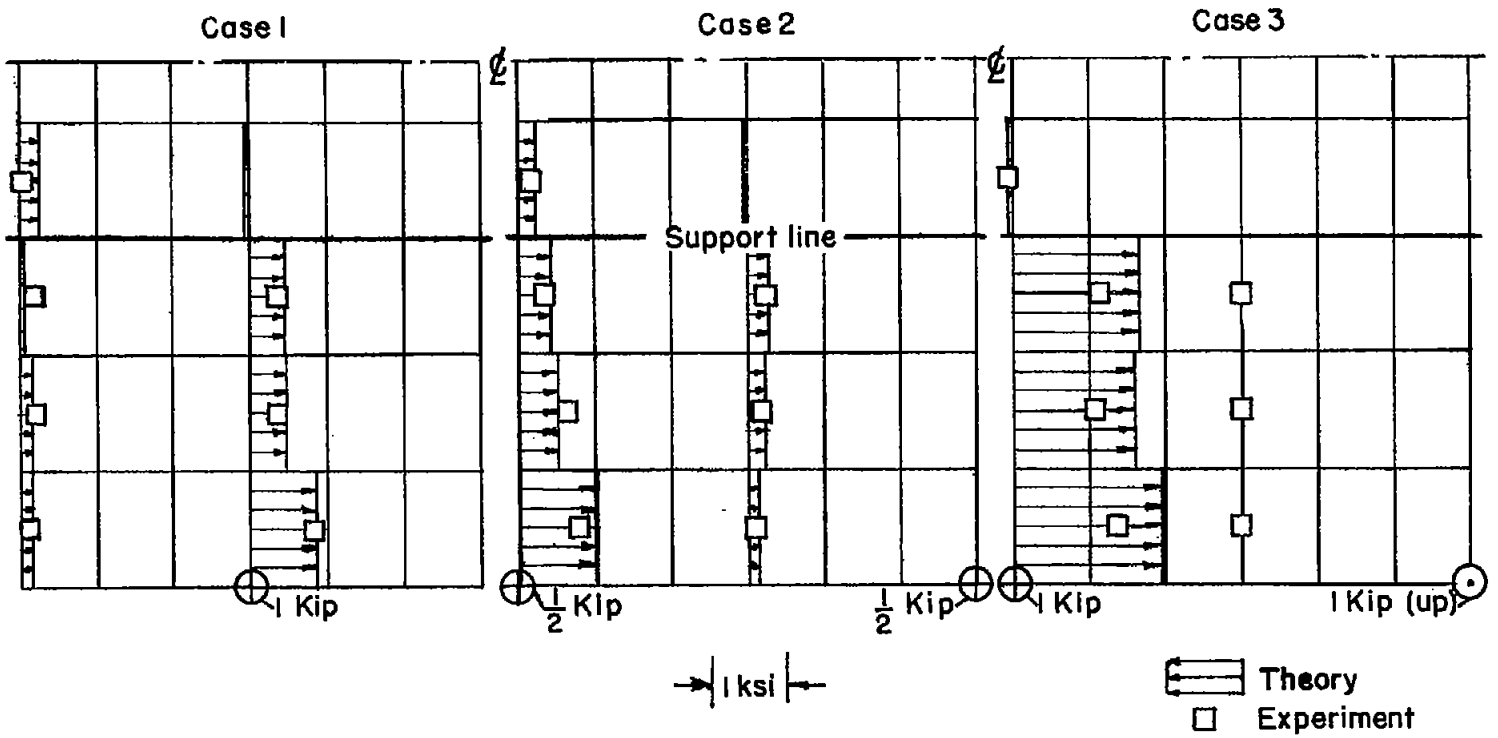

(e) Spar web shear stresses for bending and twisting loads.

Figure 6.- Concluded.

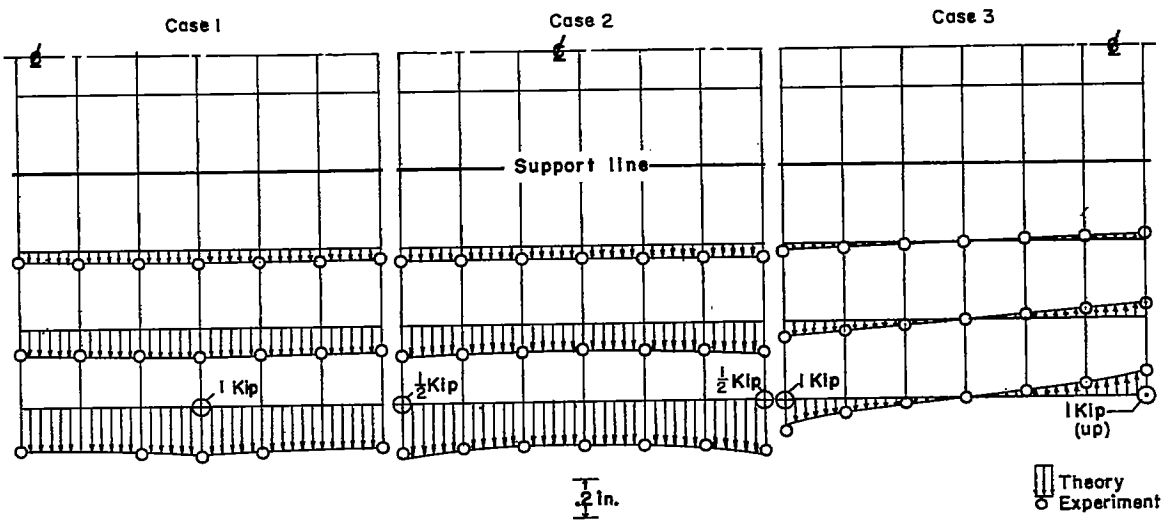

(a) Deflections for bending and twisting loads.

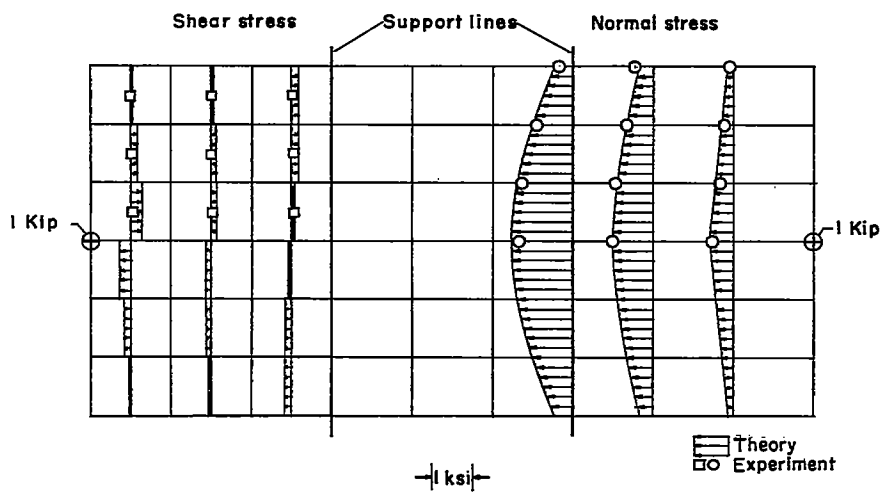

(b) Cover shear and normal stresses for loading case 1.

Figure 7.- Deflections and stresses of unswept wing with biconvex cross section.

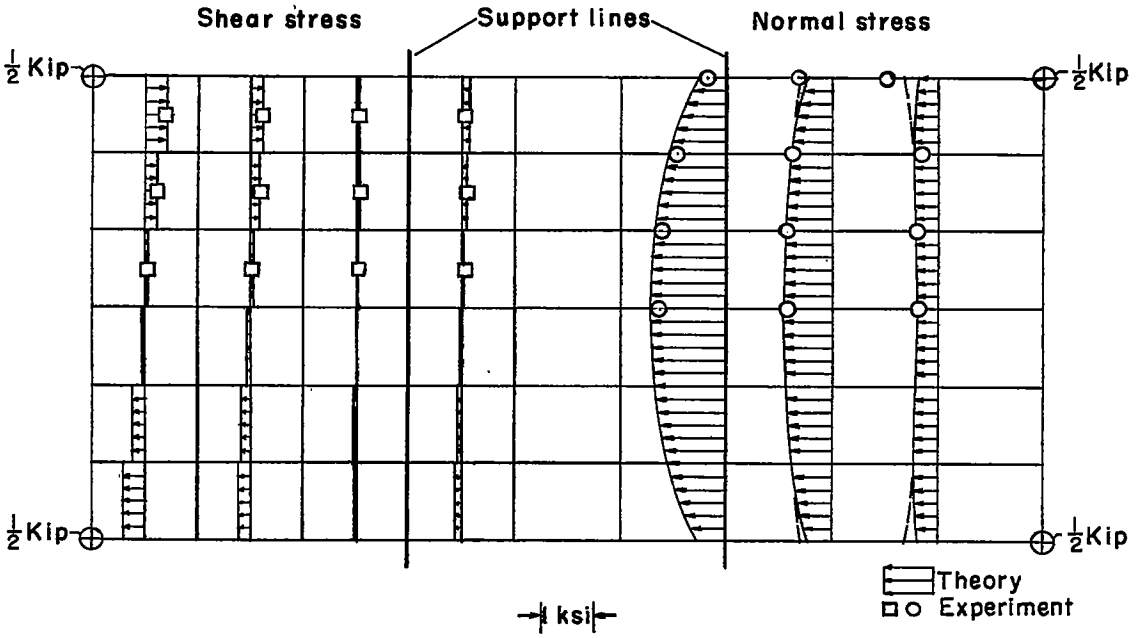

(c) Cover shear and normal stresses for loading case 2.

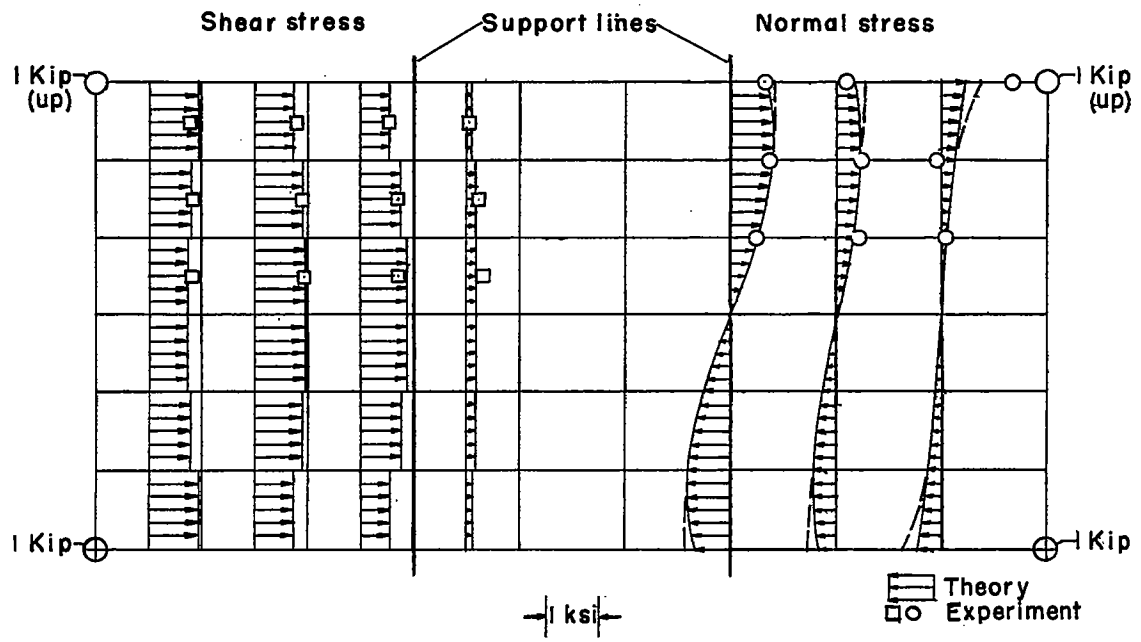

(d) Cover shear and normal stresses for loading case 3.

Figure 7.- Continued.

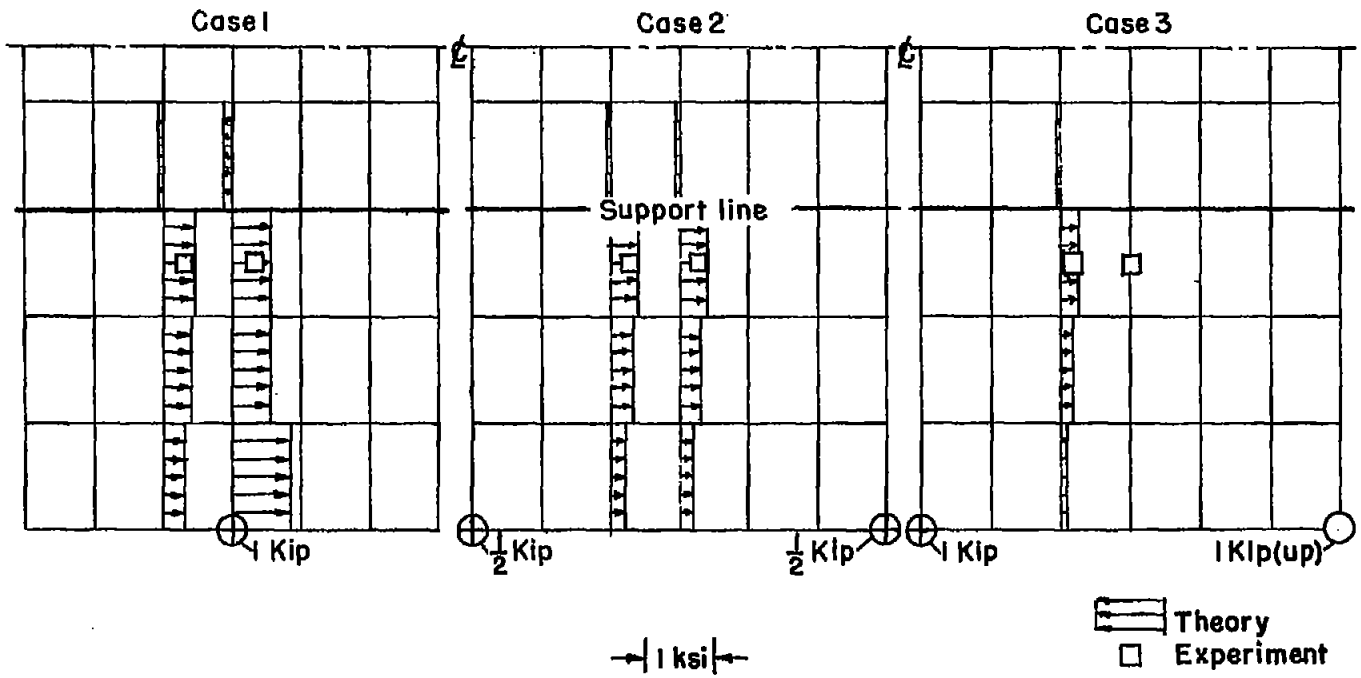

(e) Spar web shear stresses for bending and twisting loads.

Figure 7.- Concluded.

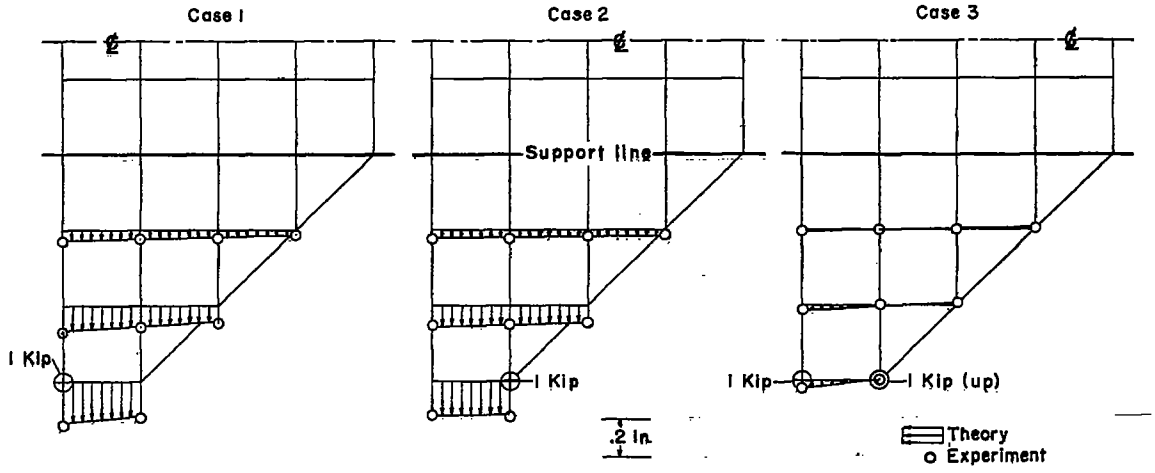

(a) Deflections for bending and twisting loads.

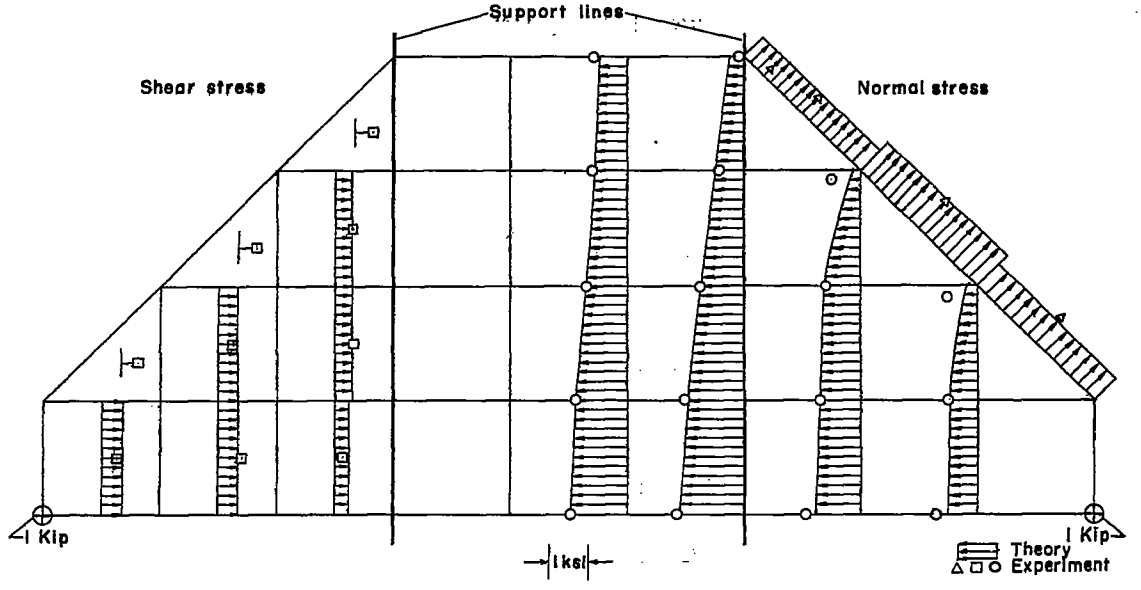

(b) Cover shear and normal stresses for loading case 1.

Figure 8.- Deflections and stresses of delta wing with rectangular cross section.

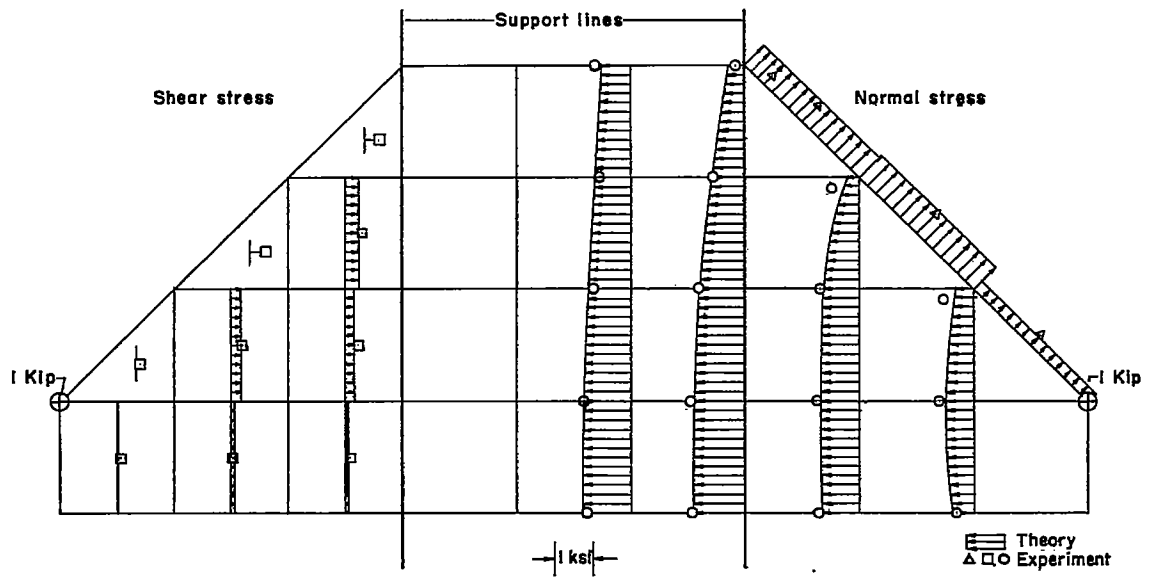

(c) Cover shear and normal stresses for loading case 2.

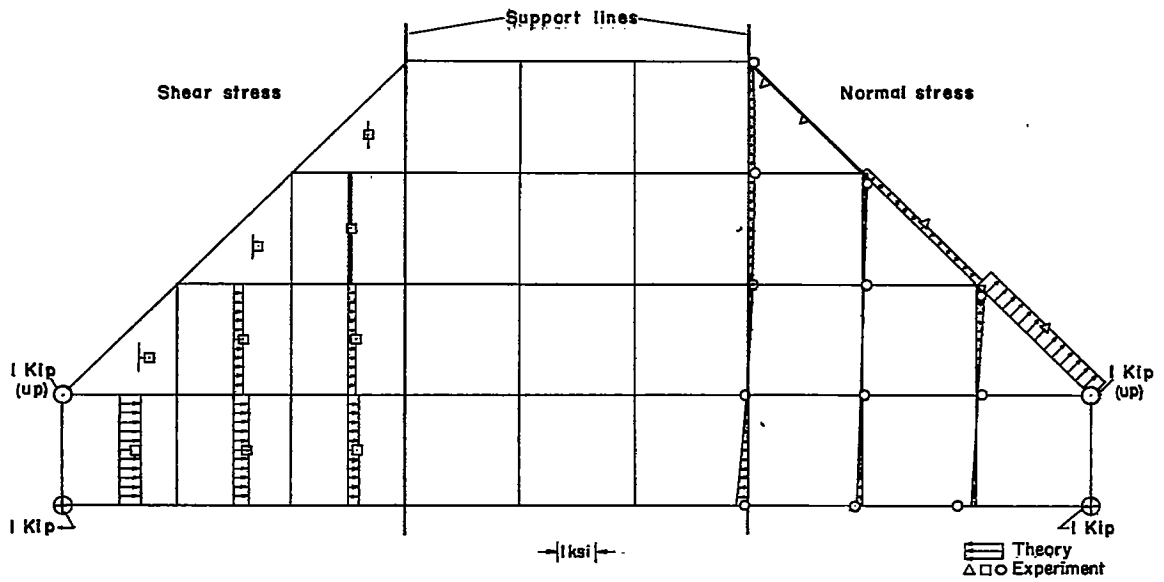

(d) Cover shear and normal stresses for loading case 3.

Figure 8.- Continued.

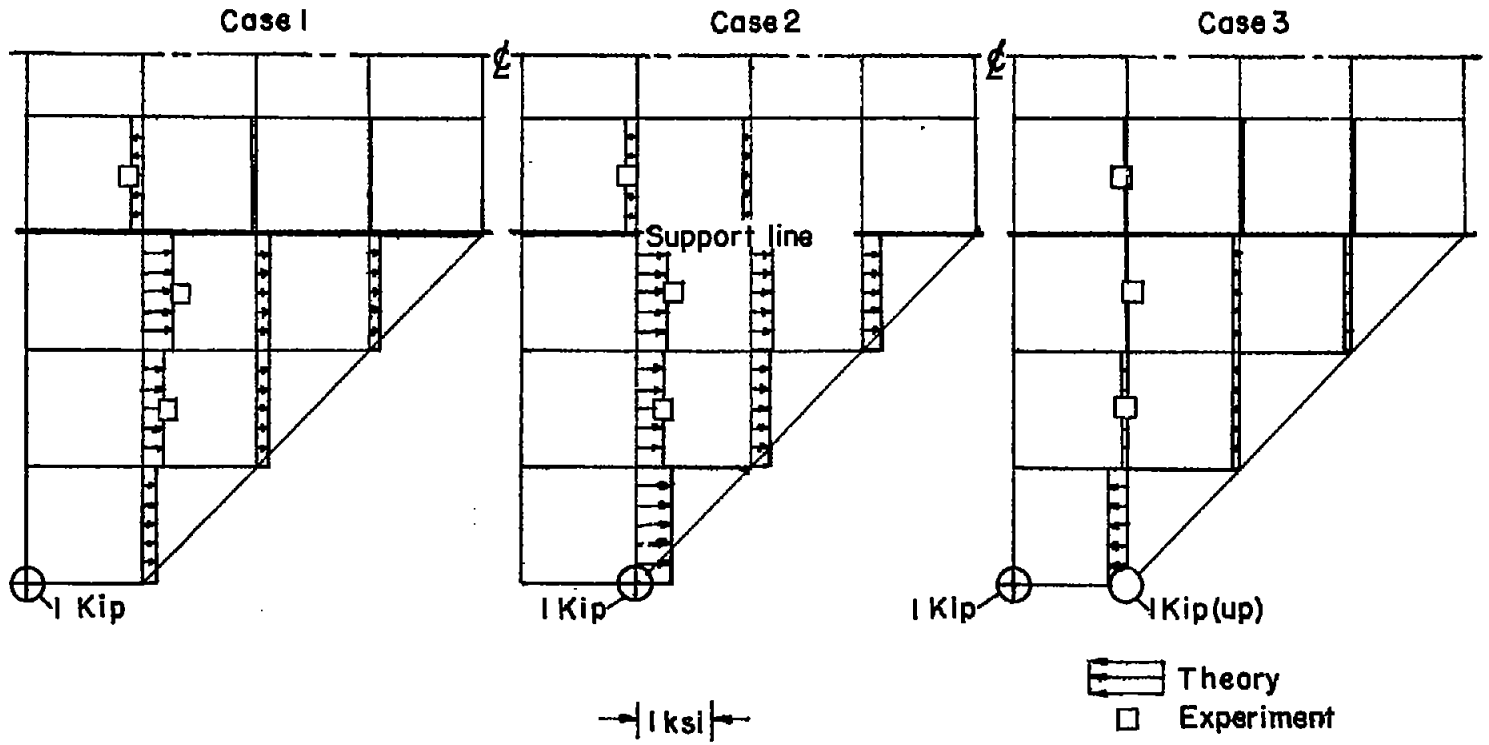

(e) Spar web shear stresses for bending and twisting loads.

Figure 8.- Concluded.

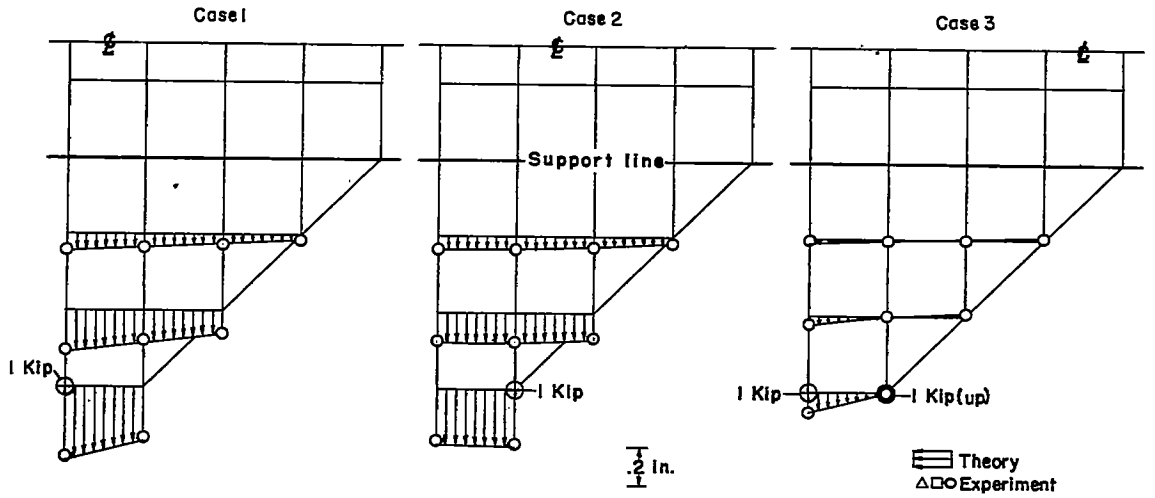

(a) Deflections for bending and twisting loads.

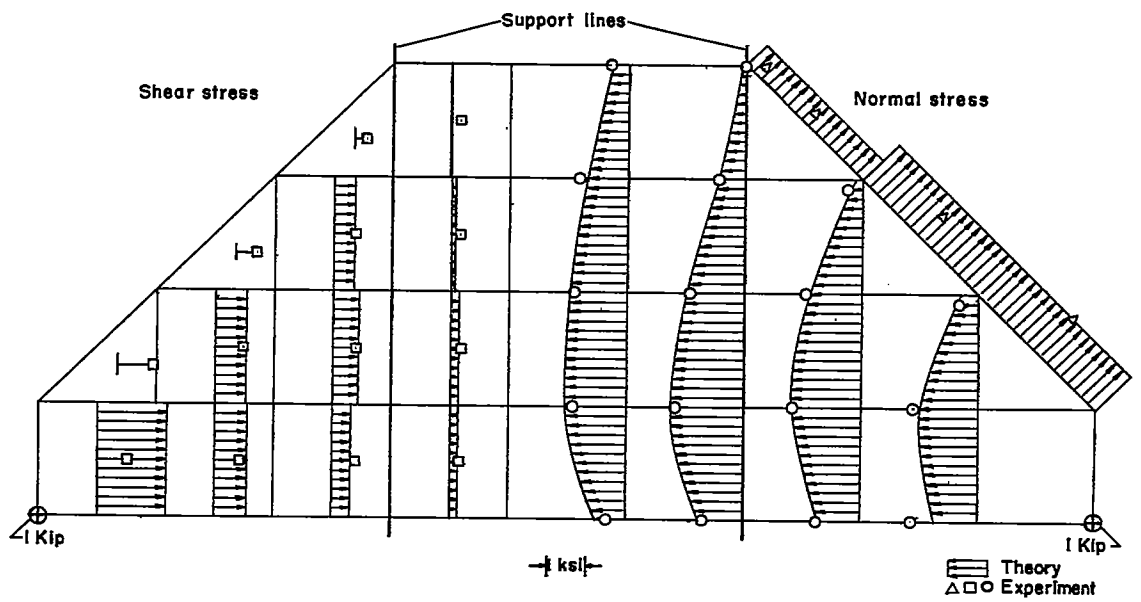

(b) Cover shear and normal stresses for loading case 1.

Figure 9.- Deflections and stresses of delta wing with biconvex cross section.

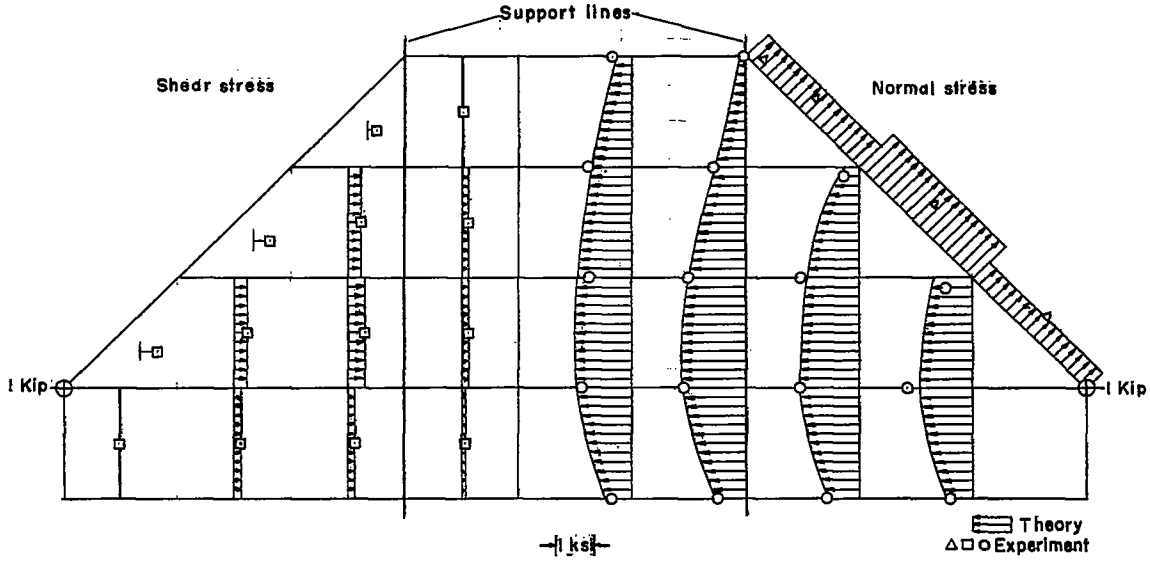

(c) Cover shear and normal stresses for loading case 2.

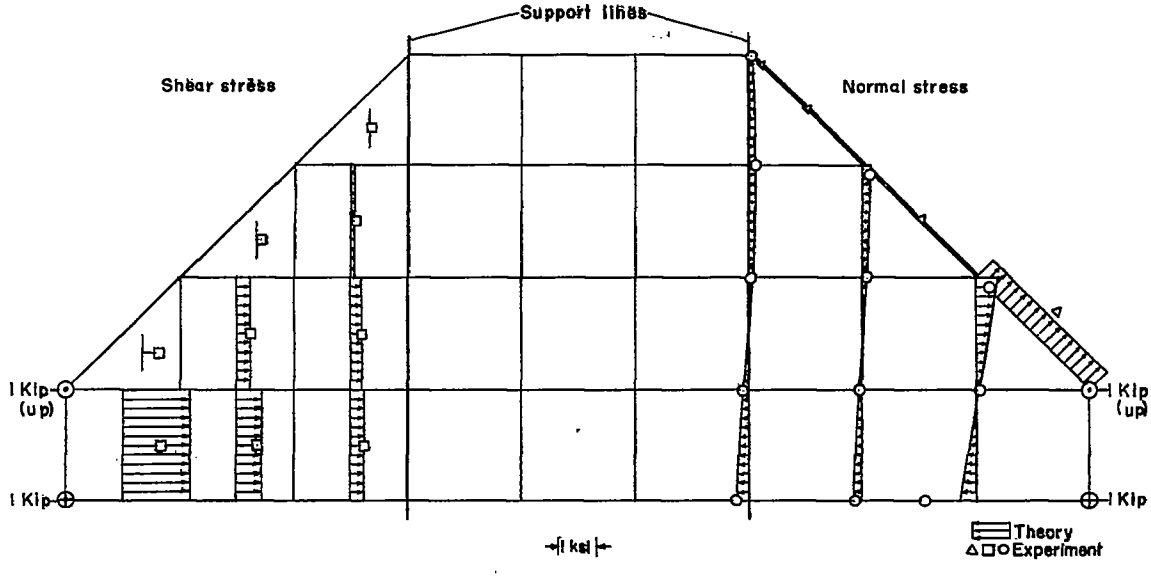

(d) Cover shear and normal stresses for loading case 3.

Figure 9.- Continued.

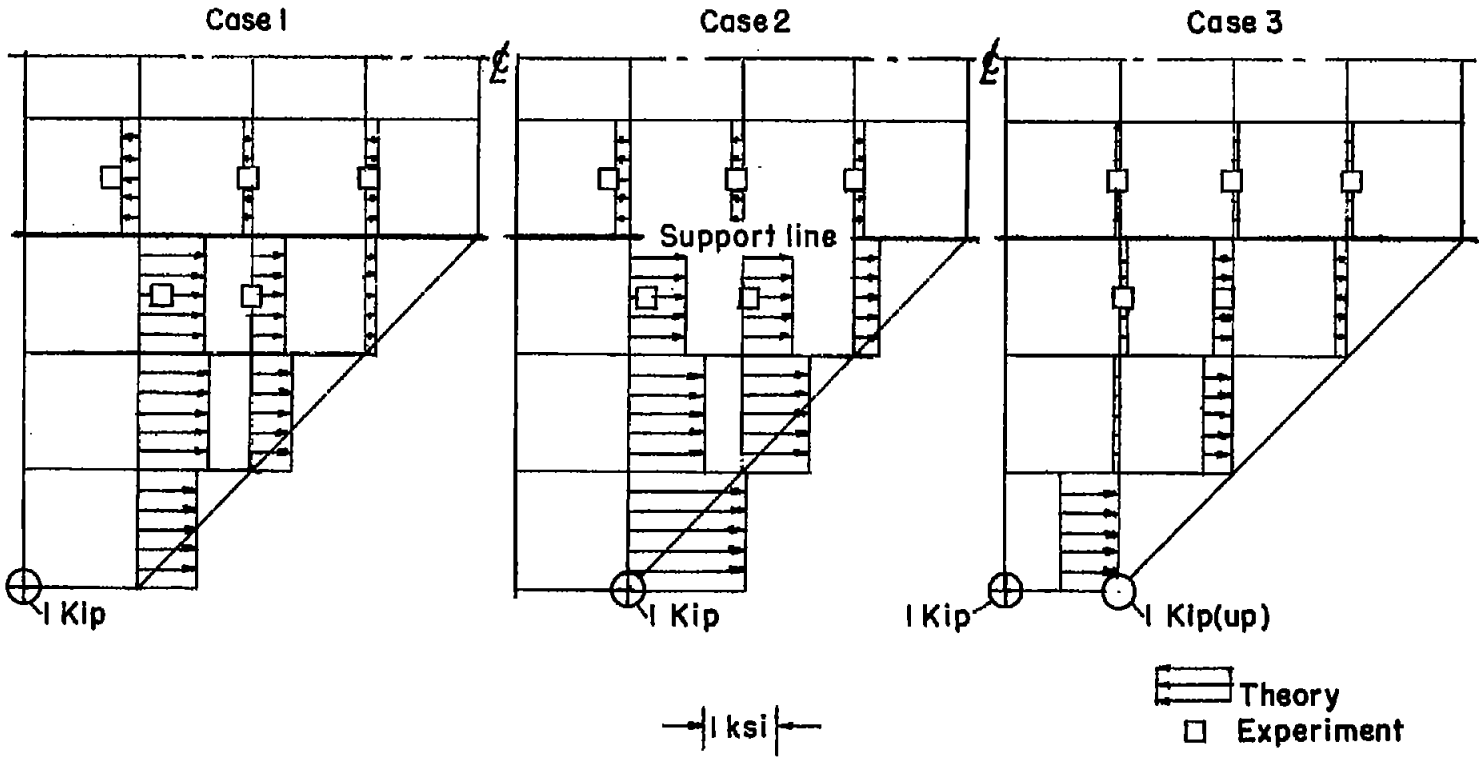

(e) Spar web shear stresses for bending and twisting loads.

Figure 9.- Concluded.

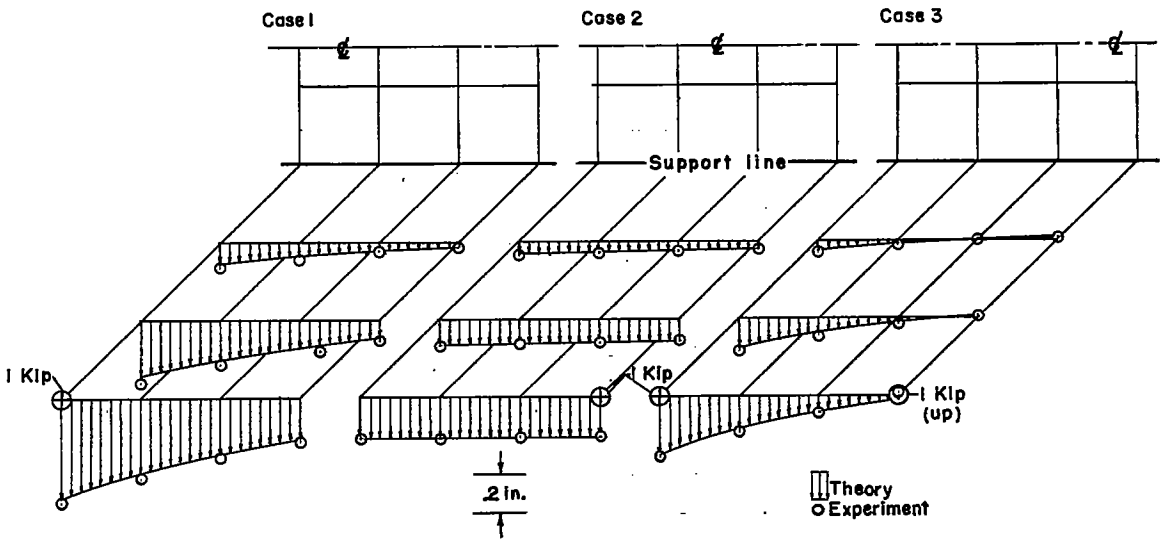

(a) Deflections for bending and twisting loads.

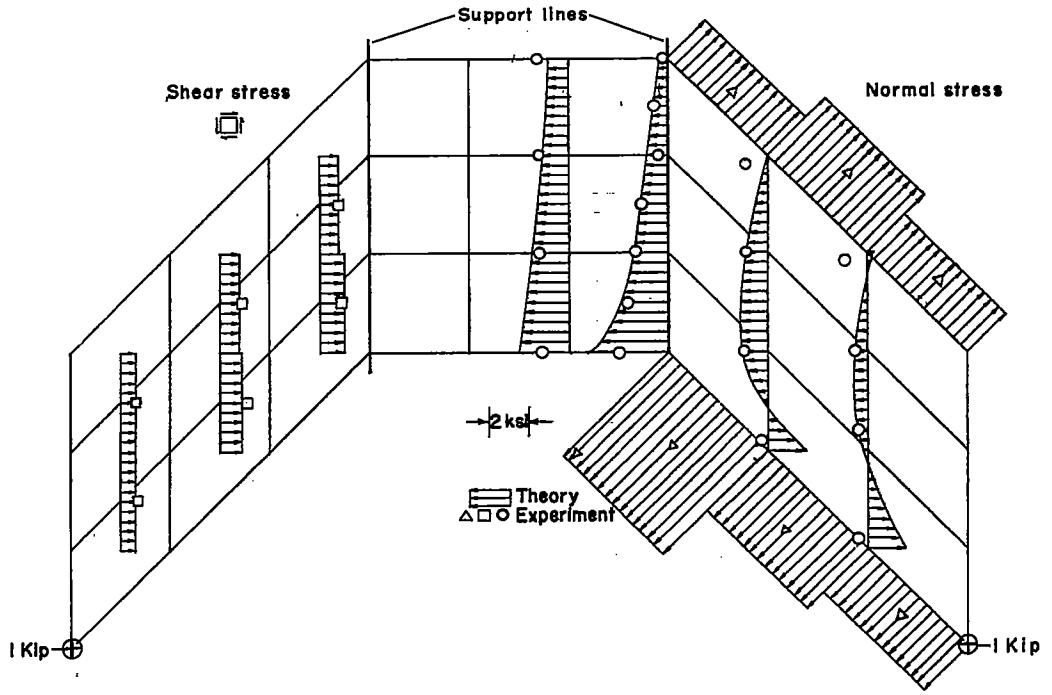

(b) Cover shear and normal stresses for loading case 1.

Figure 10.- Deflections and stresses of sweptback wing with rectangular cross section.

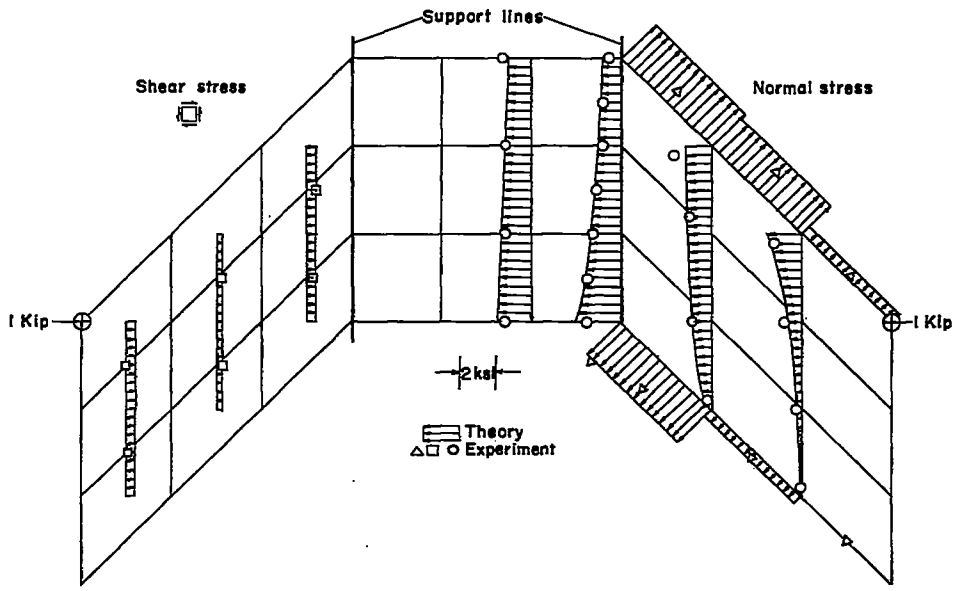

(c) Cover shear and normal stresses for loading case 2.

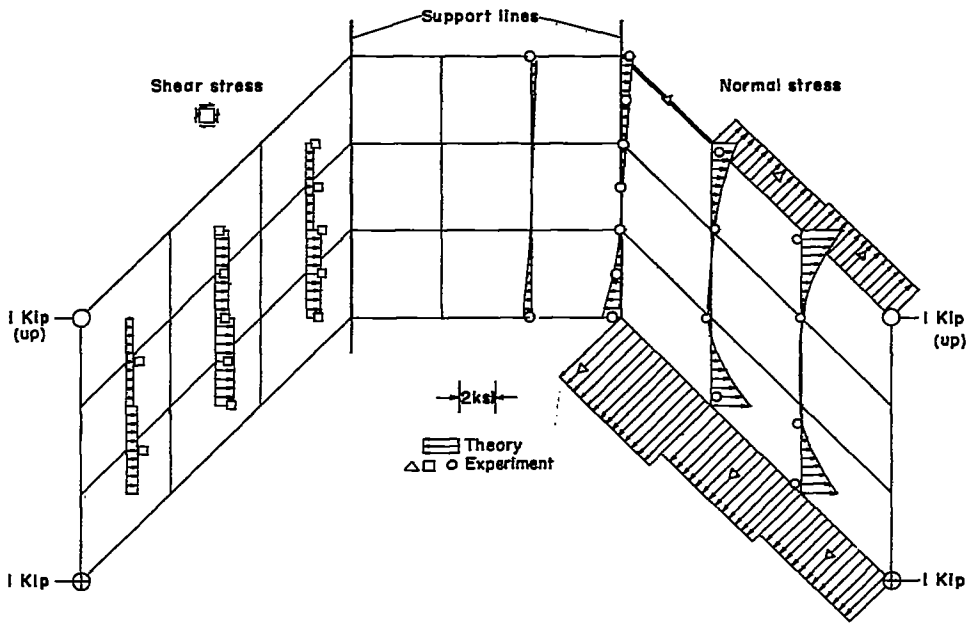

(d) Cover shear and normal stresses for loading case 3.

Figure 10.- Continued.

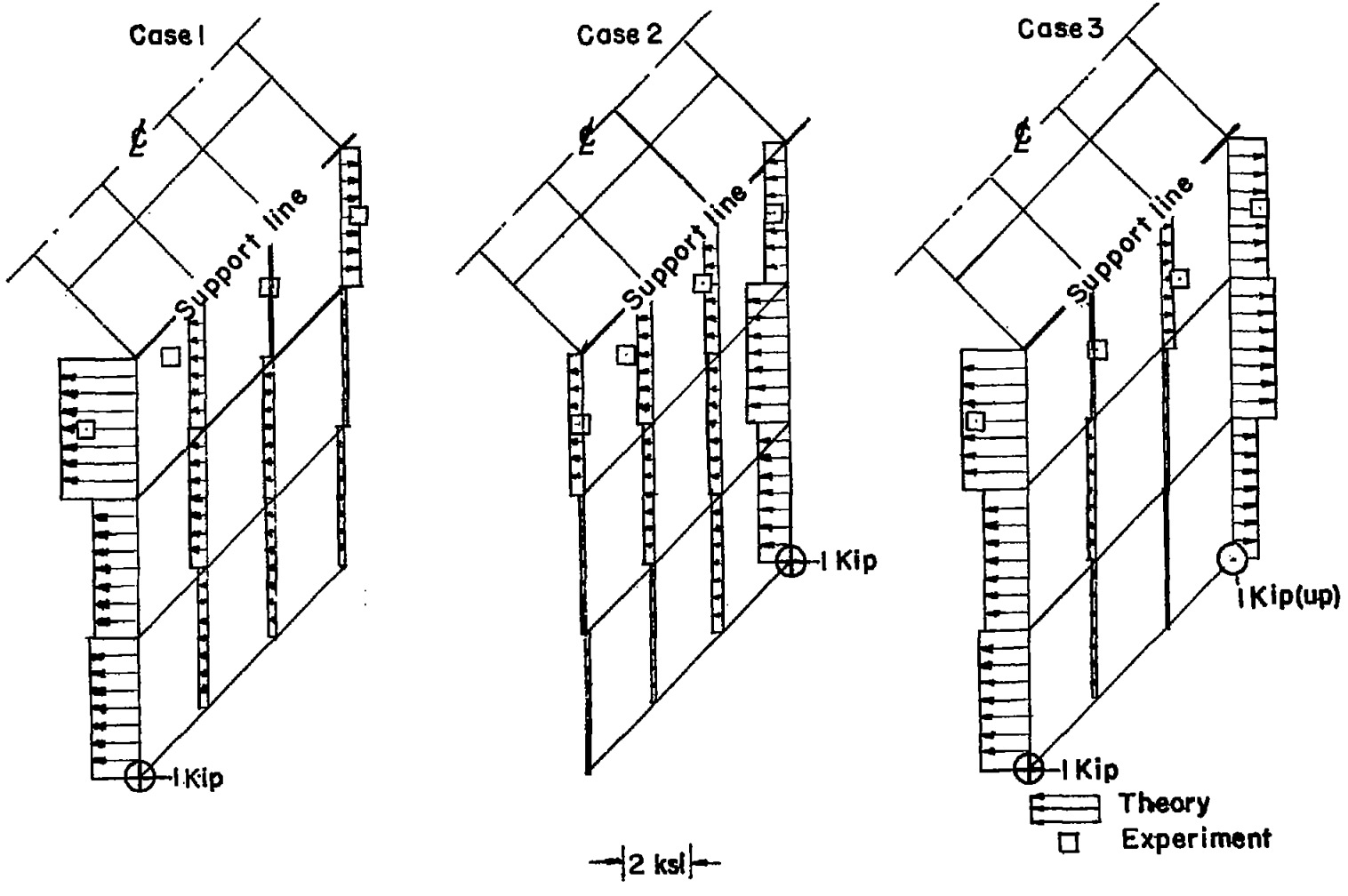

(e) Spar web shear stresses for bending and twisting loads.

Figure 10.- Concluded.

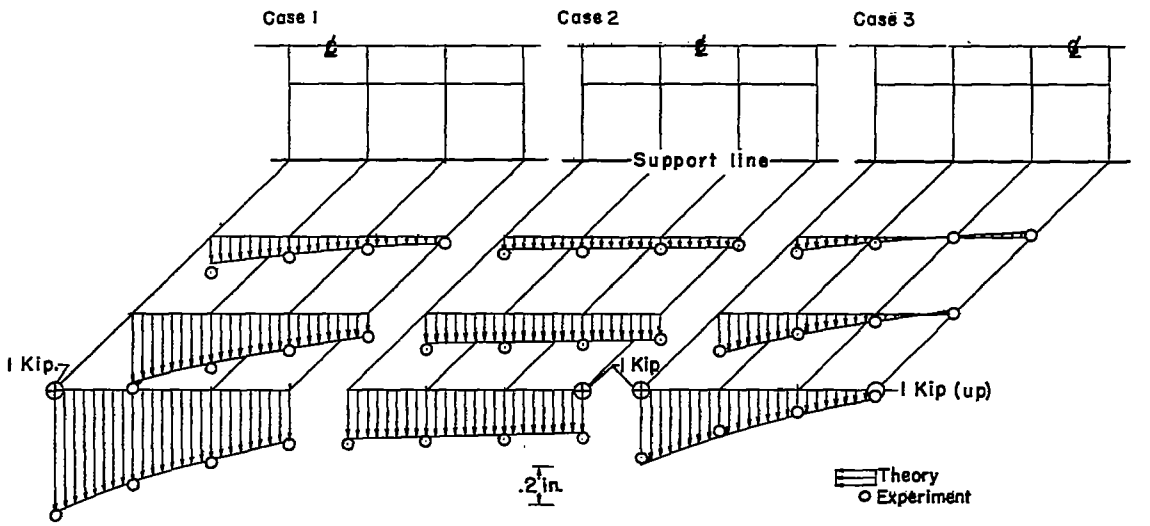

(a) Deflections for bending and twisting loads.

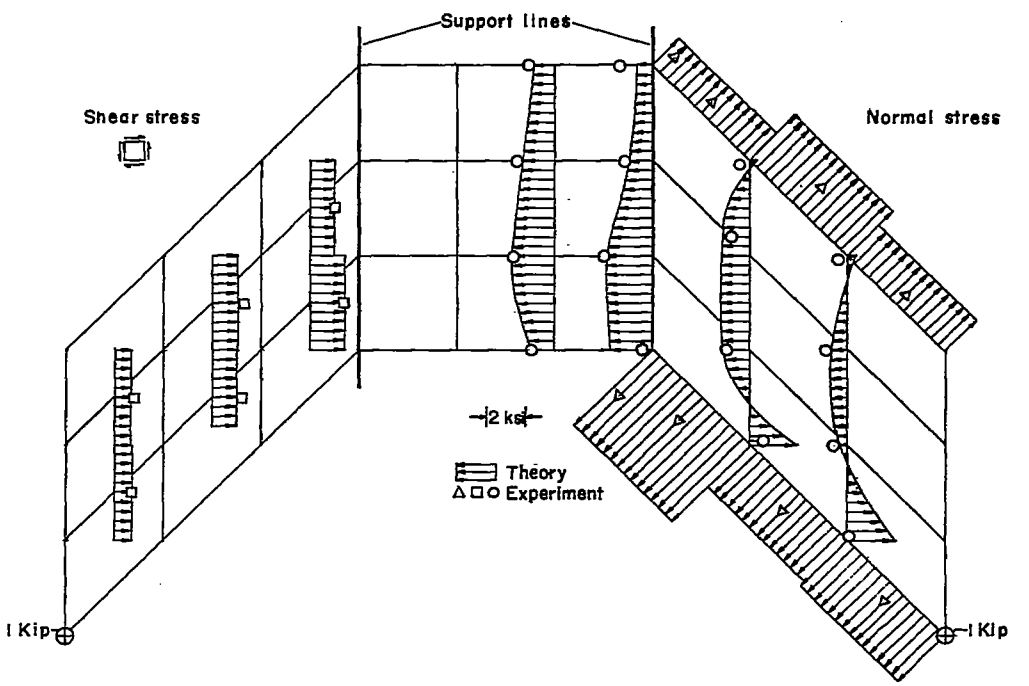

(b) Cover shear and normal stresses for loading case 1.

Figure 11.- Deflections and stresses of sweptback wing with biconvex cross section.

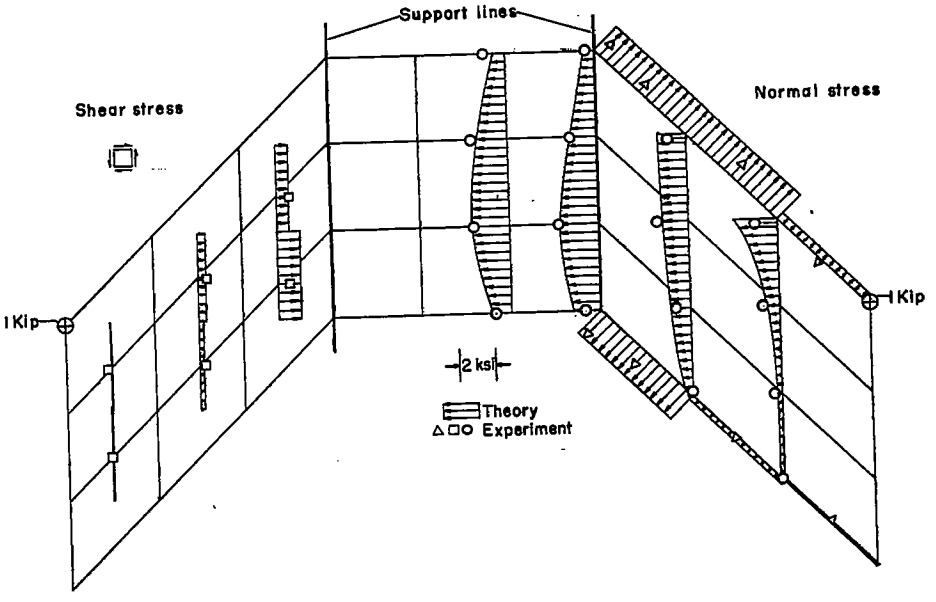

(c) Cover shear and normal stresses for loading case 2.

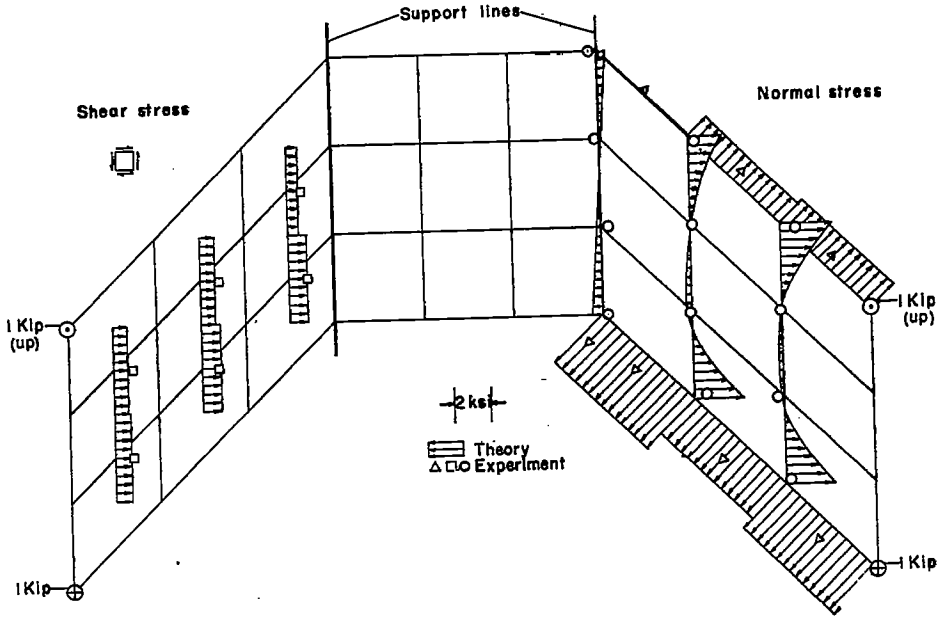

(d) Cover shear and normal stresses for loading case 3.

Figure 11.- Continued.

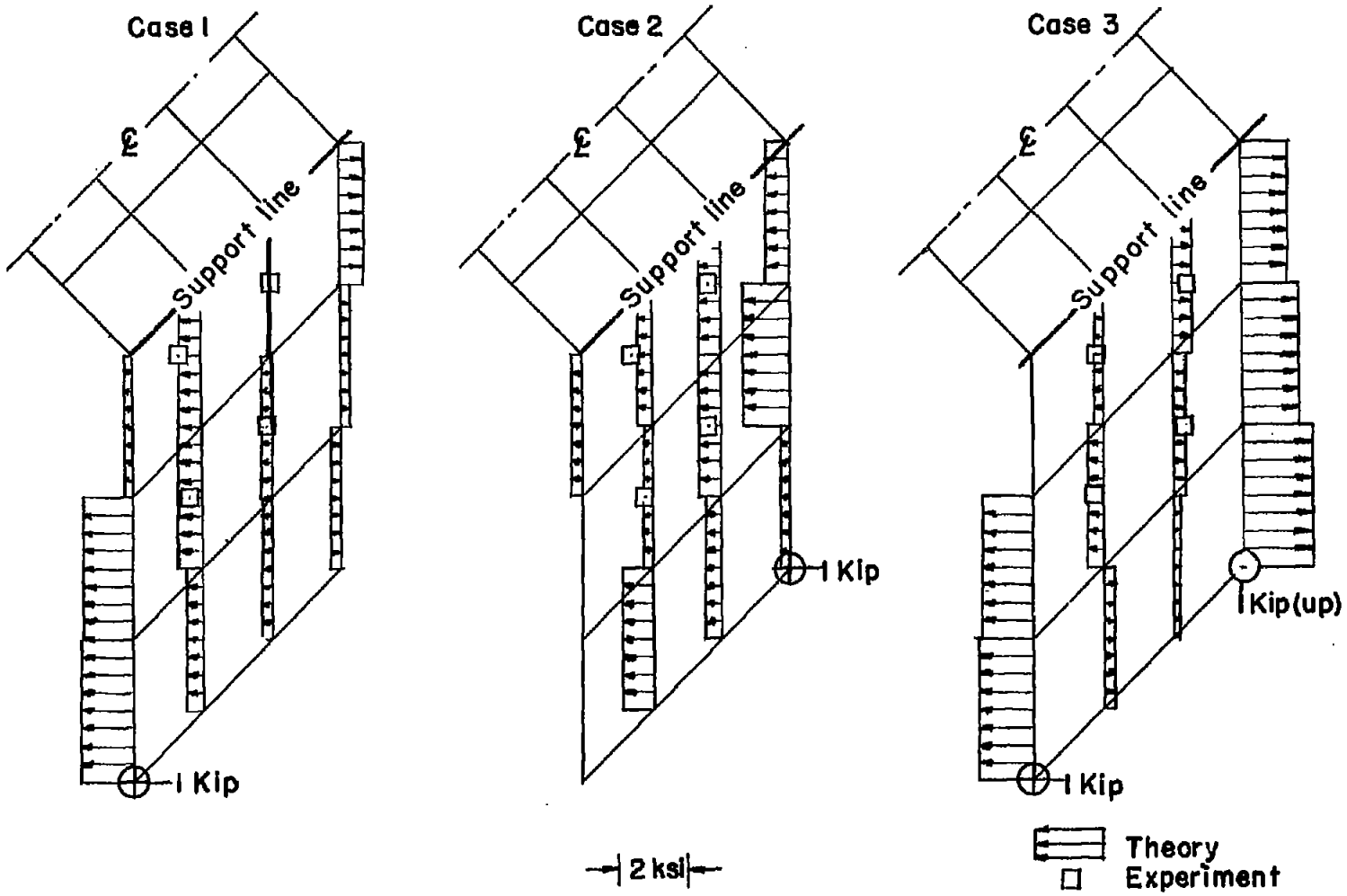

(e) Spar web shear stresses for bending and twisting loads.

Figure 11.- Concluded.

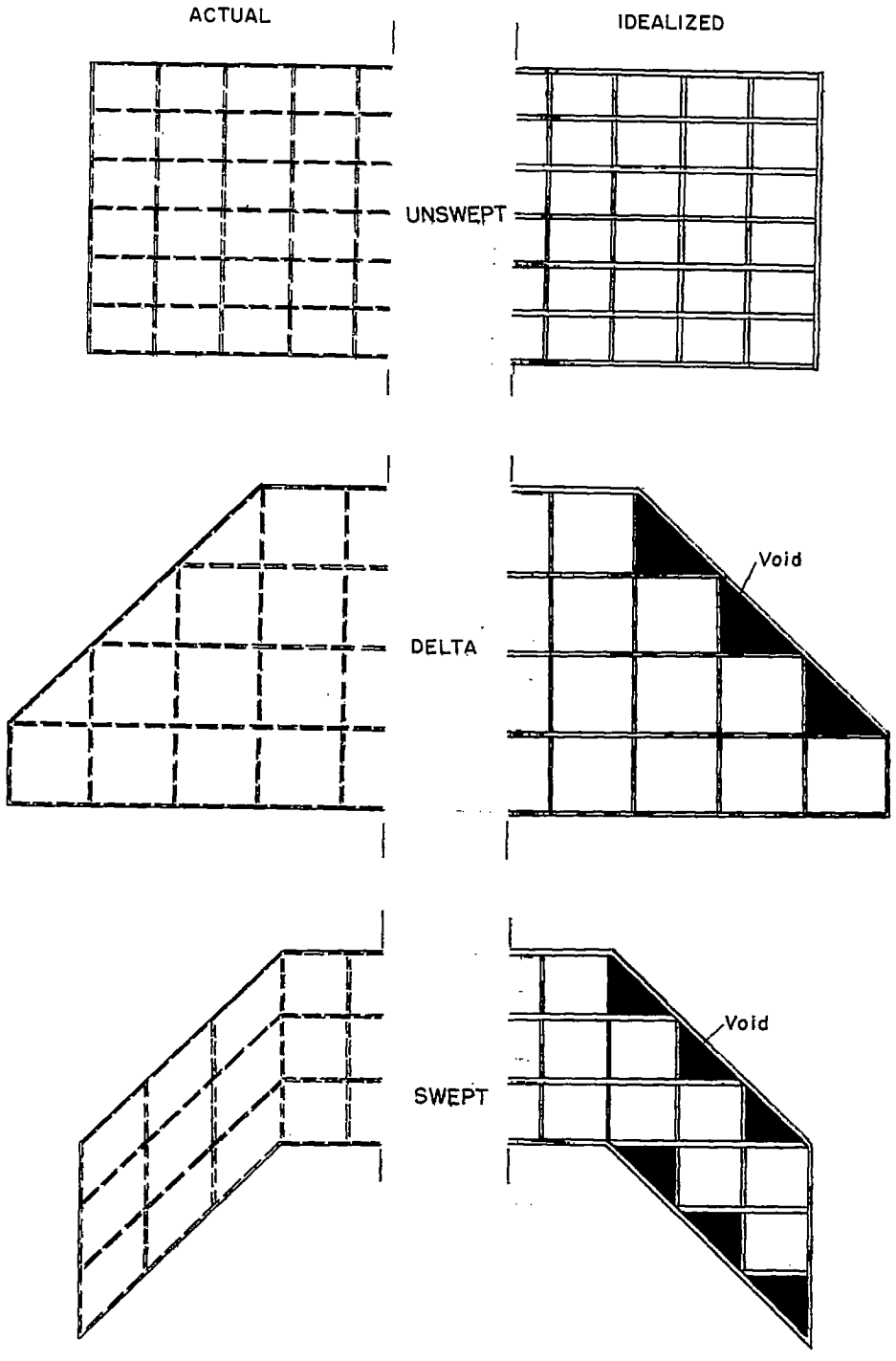

Figure 12.- Actual and idealized covers of unswept, delta, and swept plan-form wings.